EXPERIMENTAL VERIFICATION FOR CALIBRATION OF THE CONSTRAINING LINKAGE OF A 4 DEGREES OF FREEDOM MANIPULATOR

Leila Notash, Victoria Lee and Andrew Horne

Department of Mechanical and Materials Engineering, Queen's University, Kingston, ON, Canada
notash@me.queensu.ca horne@me.queensu.ca

Abstract. In this article an experimental verification for the calibration of the constraining linkage of a wire-actuated parallel robot is discussed. The experimental test bed includes a prototyped 4 degrees of freedom wire-actuated parallel manipulator and an optical tracking system. The parallel manipulator employs hybrid actuation of joints and wires and includes a rigid branch to constrain the motion of its mobile platform in roll and yaw rotations. The kinematic calibration of the rigid branch is performed. A point-to-point path is designed for the manipulator and an optical tracking system is used as an external measuring device to track a tool attached to the mobile platform and to register the manipulator poses. The deviation between the actual (measured) pose of the mobile platform and the calculated pose (via direct kinematics using the joint encoders), which could be due to errors in the kinematic parameters, actuators and sensors, is used as the error function.

Keywords: Parallel manipulator, kinematic calibration

1. INTRODUCTION

Parallel robot manipulators consist of one or more closed-loops of links and joints where the mobile platform (end effector) is connected to the base by at least two kinematic chains (legs/branches). Because of the closed-loop configuration, in parallel manipulators not all of the joints are actuated and sensed. That is, in closed-loop manipulators the majority of the joints are passive and generally unsensed. This is because for an n degrees of freedom (DOF) parallel manipulator, a minimum of n independent joints have to be actuated (and sensed). This could result in challenges during the kinematic analysis and also calibration of parallel manipulators, because the terms relating to the motion of passive (and unsensed) joints need to be eliminated from the equations using the constraints due to the closed loops.

The goal of robot kinematic calibration is to obtain an accurate kinematic model of the manipulator in terms of link and joint parameters. Calibration of parallel manipulators is performed to reduce the error in the calculated mobile platform position and orientation (pose) by identifying errors of the kinematic and joint transducer parameters. Hence, precise measurement of the mobile platform pose is required, e.g., using an external measuring device, in order to quantify the pose error.

There are three main levels of robot calibration [1] which are: joint level calibration (to identify a correct relationship between the joint transducer signal and the joint displacement), geometric calibration (to identify the kinematic relation between the joints and links based on geometric parameters of the manipulator), and non-geometric calibration (to investigate gear backlash, link/joint compliance, friction and dynamic calibration).

Robot kinematic calibration procedure consists of four steps [2]. The first step is to construct a model of the robot manipulator, i.e., to determine the relationship between the joint displacements and the end effector pose. This is usually called the forward model, where the end effector pose is expressed using the joint displacements. The second step is precise measurement of the robot end effector pose using measuring devices such as coordinate measuring machines, laser interferometry, calibration fixture or

camera. The third step is the identification of the discrepancies in the parameters of kinematic model from end effector measurements and joint displacement readings at these measured poses. The last step is to compensate for the errors in the robot controller, e.g., by modifying the control software.

Linear and nonlinear least squares techniques have been used in robot calibration to obtain estimates of the parameters to be identified. The error model based on the nonlinear manipulator kinematic model is generally differentiable. Therefore, gradient search algorithms can be applied, including steepest descent method (Newton-Raphson's algorithm), iterative non-linear least squares algorithm (Gauss-Newton algorithm), damped Gauss-Newton method (Levenberg-Marquardt algorithm), and so on.

In this article calibration of the constraining linkage of a wire-actuated parallel manipulator is performed. An optical tracking system (camera) is used to track a tool that is attached to the mobile platform of the manipulator. The tracking system identifies the pose of the manipulator with respect to the reference frame of the tracking system. The tracking system is mounted on a passive tripod, and hence, its position and orientation could be varied. The base of the manipulator is not within the workspace of the tracking system. Therefore, to identify the pose of the mobile platform with respect to the manipulator base frame, using the tracking system, another tool is defined within the workspace of the tracking system (on a nearby parallel robot, with a known pose). The transformations between the reference frame of the tracking system and the frames of the two tools are identified and utilized to calculate the pose of the manipulator with respect to its base frame. Then the collected data are used for the calibration of the constraining linkage of the manipulator using Gauss-Newton and Levenberg-Marquardt methods. The results verify the success of calibration.

2. MANIPULATOR DESCRIPTION AND MODEL

The considered wire-actuated parallel manipulator (Figure 1) has 4 DOF, and includes a rigid branch (with seven joints) and three wires [3]. The rigid branch is employed to constrain the undesired motions of the mobile platform, i.e., the roll and yaw rotations, and it connects the center of the mobile platform to the base. The rigid branch consists of a parallelogram mechanism (a 1 DOF mechanism) which is connected to the base via an actuated revolute joint (1 DOF). The coupler link of the parallelogram mechanism is connected to the mobile platform via an intermediate link and two revolute joints (2 DOF). Two joints of the rigid branch, i.e., the joints closest to the base (joints j_1 and j_2), are actuated. The two revolute joints that connect the parallelogram mechanism to the mobile platform (joints j_4 and j_5) are only equipped with encoders, i.e., these joints are not actuated. The motions of these two revolute joints are controlled by three wires as wires could only pull (not push).

Denavit-Hartenberg (DH) parameters (θ_i, d_i, a_i, α_i) [5] are used for modelling the joints of the manipulator. For the calibration model of parallel joint axes, modified Denavit-Harterberg method (θ_i, a_i, α_i, β_i) is used [6]. Table 1 includes the list of rigid branch parameters. In order to include the distance between the origins of coordinate frames for joints j_3 and j_4 (labelled in Figure 1) in the DH table, a dummy frame $X_{3'}Y_{3'}Z_{3'}$ is used. Otherwise, this distance would be along the Y_2 axis. A planar model is used for deriving the relations for the dependent joints of the parallelogram mechanism [4].

The transformation matrix between two adjacent reference frames is formed using the basic transformations as:

$$\boldsymbol{A}_{i\text{-}1,i} = \boldsymbol{Rot}(z,\theta_i)\boldsymbol{Trans}(z,d_i)\boldsymbol{Trans}(x,a_i)\boldsymbol{Rot}(x,\alpha_i) \tag{1}$$

$$\boldsymbol{A}_{i\text{-}1,i} = \boldsymbol{Rot}(z,\theta_i)\boldsymbol{Trans}(x,a_i)\boldsymbol{Rot}(x,\alpha_i)\boldsymbol{Rot}(y,\beta_i) \tag{2}$$

where equation (1) relates to the DH parameters and equation (2) corresponds to the modified DH parameters (parallel revolute joint axes of branch).

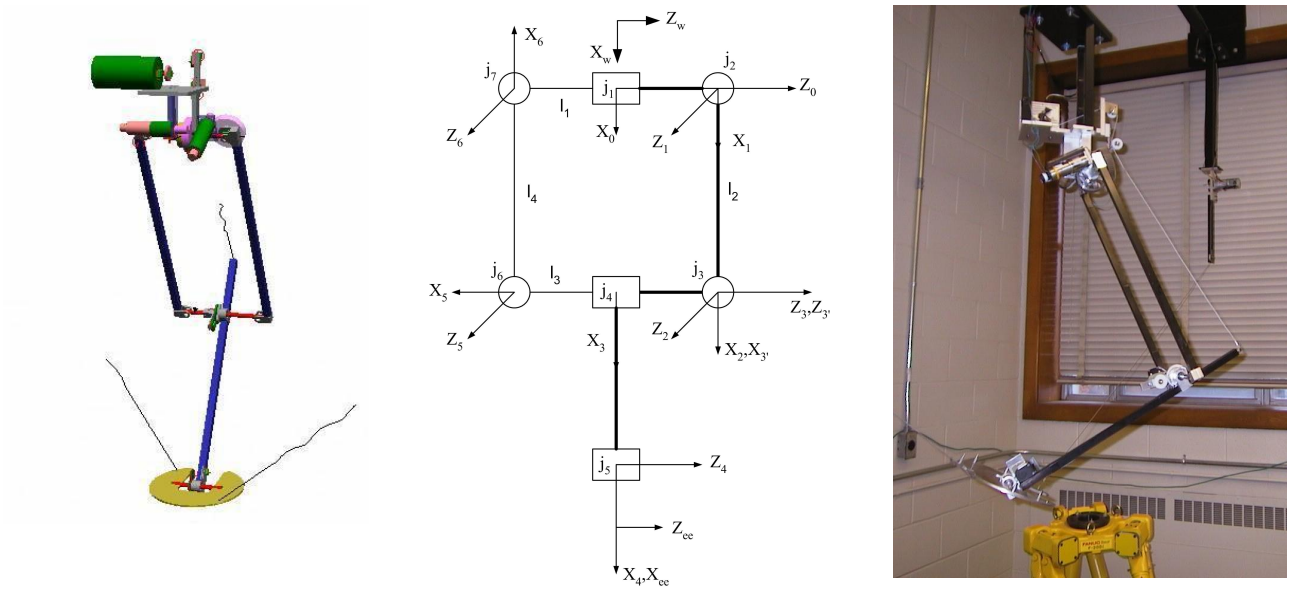

(a) (b) (c)

Figure 1: Wire-actuated manipulator: (a) solid model [3], (b) simplified diagram [4], (c) prototyped.

Table 1 Denavit-Hartenberg parameters of rigid branch.

From Frame	θ_i	d_i	a_i	α_i	β_i	To Frame
w	θ_0	0	a_0	α_0	β_0	0
0	θ_1	d_1	a_1	α_1	0	1
1	θ_2	0	$a_2 = l_2$	α_2	β_2	2
2	θ_3	0	a_3	α_3	0	3′
3′	0	$d_{3'}$	0	0	0	3
3	θ_4	0	a_4	α_4	β_4	4
4	θ_5	0	a_5	α_5	β_5	ee

The actuators of the manipulator are controlled using a Q8 data acquisition board (from Quanser Consulting Inc.), which is installed on the motherboard of a Pentium III\1.0 GHZ host computer, and WinCon^{TM} real-time Windows 2000/XP based software. The encoders of the actuated joints have a resolution of 500 pulses per revolution (ppr). The motors that are used to actuate these joints have an internal gear reduction ratio of 134:1, and an external gear transmission is used with a gear ratio of 4:1. Therefore, the resolution of these two encoders is 268,000 ppr. The resolution of the encoders of the passive joints four and five (j_4 and j_5 in Figure 1) are respectively 1000 and 200 cycles per revolution (with four pulses per one cycle). An external gear transmission is used for these two encoders, where the gear ratio for joint four is 1.6:1 and for joint five is 0.997:1. The data acquisition system has quadrature

mode, i.e., for joints four and five it could get 6400 and 797.6 counts per revolution after the quadrature decoding.

The root-mean-square (RMS) volumetric acceptance criterion for the Polaris tracking system (from Northern Digital Inc.) is reported to be 0.350 mm (based on a single marker stepped through over 1200 positions throughout the defined workspace, using the mean of 30 samples at each position, at 20°C) [7]. The resolutions of the encoders and the RMS error of the tracking system dictate the accuracy level of the calibration.

3. MANIPULATOR PARAMETER IDENTIFICATION

Due to the manufacturing (fabrication and assembly) tolerances and also non-geometric errors such as gear backlash, there is an inconsistency between the measured mobile platform pose $\boldsymbol{r}$ and the pose obtained from kinematic model $\boldsymbol{r}_c(\boldsymbol{q},\boldsymbol{a})$. The error vector of mobile platform pose in the jth measurement can be formulated as

$$\boldsymbol{e}_j = \boldsymbol{r}_j - \boldsymbol{r}_c(\boldsymbol{q}_j, \boldsymbol{a}) \tag{3}$$

where $\boldsymbol{r}_j$ is the mobile platform pose in the jth measurement, $\boldsymbol{q}_j$ is the vector of joint displacements, and $\boldsymbol{a}$ is the vector of kinematic parameters. The objective is to identify the discrepancies in the kinematic and joint parameters such that the following expression is minimized for all manipulator poses

$$\sum_{j=1}^{m} \boldsymbol{e}_j^T \boldsymbol{e}_j \tag{4}$$

where m is the total number of measured mobile platform poses. Expression (4) is a nonlinear function of kinematic and joint parameter errors. This expression could be linearized using the Taylor series expansion, or a nonlinear function minimization approach may be employed to identify the desired errors.

For the linearized model (Gauss-Newton approach, GN), assuming small errors, i.e., neglecting the second and higher order differential terms, the error vector reduces to

$$\boldsymbol{e}_j = \frac{\partial \boldsymbol{r}_c(\boldsymbol{q}_j, \boldsymbol{a})}{\partial \boldsymbol{q}} \delta\boldsymbol{q} + \frac{\partial \boldsymbol{r}_c(\boldsymbol{q}_j, \boldsymbol{a})}{\partial \boldsymbol{a}} \delta\boldsymbol{a} \tag{5}$$

Equation (5) is linear with respect to the parameter errors $\delta\boldsymbol{a}$ and joint errors $\delta\boldsymbol{q}$. The mobile platform pose error for all of the measured poses can be written as

$$\boldsymbol{e}_{ag} = \begin{bmatrix} \boldsymbol{J}_1 \\ \vdots \\ \boldsymbol{J}_m \end{bmatrix} \begin{bmatrix} \delta\boldsymbol{q} \\ \delta\boldsymbol{a} \end{bmatrix} = \boldsymbol{J}_{ag} \delta\boldsymbol{c}_{ag} \tag{6}$$

where $\boldsymbol{e}_{ag} = \begin{bmatrix} \boldsymbol{e}_1^T & \cdots & \boldsymbol{e}_m^T \end{bmatrix}^T$, $\boldsymbol{J}_{ag}$, $\delta\boldsymbol{c}_{ag}$ are respectively the $6m \times 1$ aggregated mobile platform pose error, the $6m \times p$ aggregated identification Jacobian matrix and the $p \times 1$ aggregated vector of parameter errors, and $\boldsymbol{J}_j$ is the identification Jacobian matrix at the jth measurement. The least-squares solution of equation (6) is the set of parameters which minimizes $\left(\boldsymbol{e}_{ag} - \boldsymbol{J}_{ag}\delta\boldsymbol{c}_{ag}\right)^T \left(\boldsymbol{e}_{ag} - \boldsymbol{J}_{ag}\delta\boldsymbol{c}_{ag}\right)$ and can be obtained as

$$\delta\boldsymbol{c}_{ag} = \boldsymbol{J}^+ \boldsymbol{e}_{ag} \tag{7}$$

where $\boldsymbol{J}_{ag}^+ = \left(\boldsymbol{J}_{ag}^T \boldsymbol{J}_{ag}\right)^{-1} \boldsymbol{J}_{ag}^T$ is the generalized inverse of $\boldsymbol{J}_{ag}$. For an improved result, this approach should be iteratively repeated.

The Levenberg-Marquardt (LM) method, which is based on the gradient vector and Hessian matrix of the objective function, is used for the non-linear model

$$\left(\boldsymbol{J}_k^T \boldsymbol{J}_k + \mu_k \boldsymbol{I}\right)\boldsymbol{v}_k = \boldsymbol{J}_k^T (\boldsymbol{e}_{ag})_k \tag{8}$$

where $\boldsymbol{J}_k$ is the $6m \times p$ identification Jacobian of the mobile platform pose error function, $\mu \geq 0$ is a scalar, $\boldsymbol{I}$ is a $p \times p$ identity matrix, and vector $\boldsymbol{v}_k$ indicates the direction of search at the *k*-th iteration [8].

4. EXPERIMENT DESIGN

The joint level calibration is performed by calculating the gains of the encoders based on the quadrature mode of data acquisition board, resolution of the encoders and gear reduction ratios as discussed in Section 2. That is, the displacements θ of joints one, two, four and five in terms of the corresponding encoder signal η are respectively

$$\theta_1 = \frac{2\pi}{4 \times 500 \times 134 \times 4}\eta_1 \tag{9}$$

$$\theta_2 = \frac{-2\pi}{4 \times 500 \times 134 \times 4}\eta_2 \tag{10}$$

$$\theta_4 = \frac{2\pi}{4 \times 200 \times 1.690}\eta_4 \tag{11}$$

$$\theta_5 = \frac{-2\pi}{4 \times 200 \times 0.997}\eta_5 \tag{12}$$

For the kinematic calibration, the pose of the mobile platform could be fully described by the readings of the four encoders of the rigid branch, i.e., the two encoders of the actuated joints (j_1 and j_2) and the two encoders of the passive joints (j_4 and j_5). As well, the pose of the mobile platform could be measured by an external measuring device such as a Polaris optical tracking system by placing markers on the mobile platform. The emitted infrared light of the position sensor of the tracking system is reflected back by the markers to the optical receptors. Based on the reflected infrared light, the poses of markers, and hence the pose of mobile platform, are identified.

Designing the relative distances between the markers and the reference frame for the markers is called tool characterizing. The markers of the characterized tool should form a unique geometry so that the tracking system could identify the tool and find its pose. That is, minimum of three markers are required, each pair of markers being apart by at least 50 mm while the distance between any two markers is different than the others by at least 5 mm [9].

For the wire-actuated parallel manipulator, three markers (*A*, *B* and *C*) are used on the mobile platform. The origin of mobile platform frame (tool) lies on the plane of mobile platform. It should be noted that the plane passing through the centers of the three markers, which is parallel to the plane of mobile platform, is shifted by 24.5 mm in $-Y_{ee}$ direction. As depicted in Figure 2(a), the origin of $X_{ee}Y_{ee}Z_{ee}$ frame is below marker *A* with Y_{ee} axis being normal to the plane of markers. The axes of the mobile platform frame are parallel to the fixed frame $X_0Y_0Z_0$ at the base of the manipulator when the constraining linkage is fully extended downward and the mobile platform plane is horizontal. The pose of the mobile platform frame is identified by these three markers, positioned on the mobile platform based on the requirements of the NDI Architect software of Polaris for defining the tools to be tracked. The coordinates of these markers with respect to frame $X_{ee}Y_{ee}Z_{ee}$ are as follows: *A* (0, –24.500, 0), *B* (–34.231, –24.500, –84.272), and *C* (–118.570, –24.5, 118.569). The tracking system uses the three markers and reports the pose of frame $X_{ee}Y_{ee}Z_{ee}$.

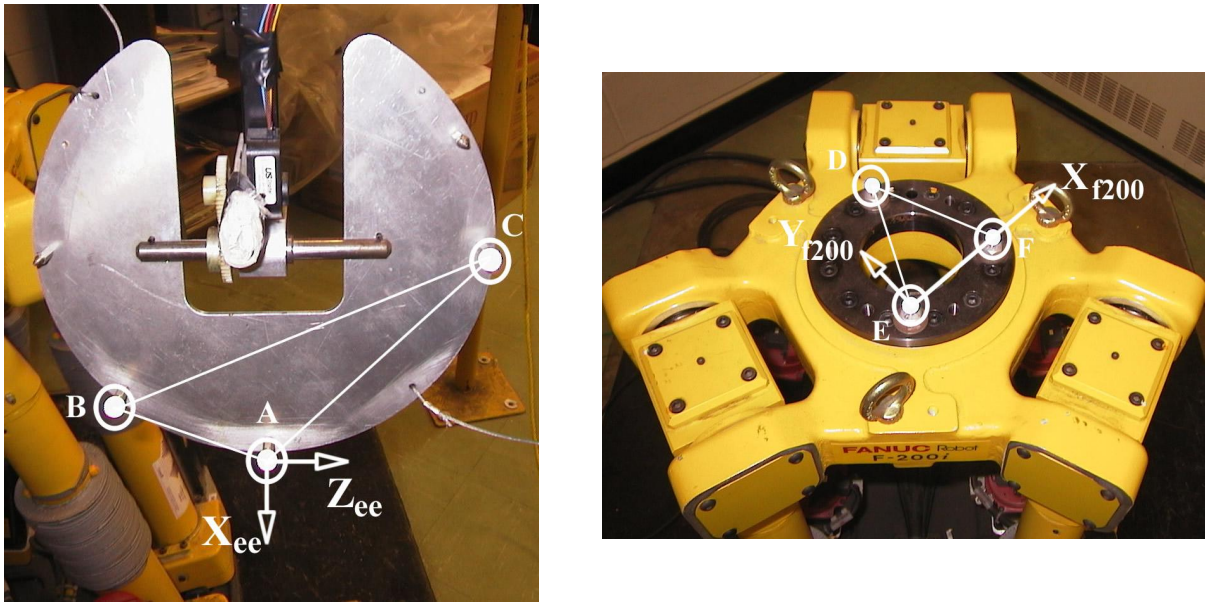

(a) (b)

Figure 2: Three passive markers on mobile platform of (a) wire-actuated manipulator, (b) F200*i* robot.

In order to obtain the mobile platform pose with respect to the base coordinate frame, two tools are needed, one on the mobile platform of the wire-actuated manipulator and one to define the base (global) frame. The reference frame of the tracking system is not used for the measurements as Polaris is mounted on a passive tripod where its position and orientation could be varied (will not be the same for different measurements in case it is moved during experiment and data collection). Because the base of the wire-actuated manipulator is not accessible for putting markers and also it does not lie within the workspace of Polaris, a tool is defined on another parallel manipulator (FANUC F200*i*) which is located below the wire-actuated parallel manipulator. The mobile platform of F200*i* parallel robot at its home position (when the lengths of its prismatic joints are 668mm) is within the workspace of Polaris. The tool of F200*i* is also characterized by three markers. As illustrated in Figure 2(b), the plane of markers is defined as XY plane, which is about 22.7 mm above the mobile platform plane of F200*i*. The origin of the reference frame is located at the center of marker *E* with markers *E* and *F* positioned on the X_{f200} axis. The coordinates of these markers with respect to the $X_{f200}Y_{f200}Z_{f200}$ frame are as follows: *D* (60.255, 104.691, 0), *E* (0, 0, 0), and *F* (87.893, 0, 0).

As mentioned earlier, the deviation between the measured pose of the mobile platform of the wire-actuated parallel manipulator and the calculated pose (via direct kinematics using the joint encoders) is used as the error function. The manipulator poses are selected uniformly within its workspace. The optical tracking system is used to follow the mobile platform of the wire-actuated manipulator and display the pose (roll, pitch, yaw, p_x, p_y p_z) with respect to the reference frame which was defined on the mobile platform of the F200*i* (global frame). The transformations between the base and the mobile platform frames of the manipulator and the global frame were modelled and identified as follows.

Using Polaris measurements of the two tools (one on the wire-actuated manipulator, one on the F200*i* robot) and the known pose of the wire-actuated manipulator at certain configurations based on the nominal values of its parameters, e.g., its zero-configuration when all joint displacements are zero), the measured pose of the wire-actuated manipulator with respect to the F200*i* tool are converted to the corresponding poses relative to the base coordinate frame of the manipulator. The constant transformation

from the base frame of wire-actuated parallel manipulator to the tool on F200*i* (at its home position), $\boldsymbol{A}_{0,F200}$, is determined experimentally using

$$\boldsymbol{A}_{0,ee} = \boldsymbol{A}_{0,F200}\,\boldsymbol{A}_{F200,ee} \tag{13}$$

where the mobile platform pose of manipulator with respect to its base frame, $\boldsymbol{A}_{0,ee}$, is calculated for the nominal DH parameters of the rigid branch for the known poses of manipulator. The relative position of the tool of wire-actuated manipulator with respect to the tool of F200*i*, $\boldsymbol{A}_{F200,ee}$, is measured by Polaris. The measurements are carried out for six different poses of manipulator (Table 2) and the calculated six poses (pitch angle and three translational coordinates) of the F200*i* tool with respect to the base frame, based on $\boldsymbol{A}_{0,F200}$, are used to define the constant transformation $\boldsymbol{A}_{0,F200}$. For example, the transformation matrices $\boldsymbol{A}_{F200,ee}$ and $\boldsymbol{A}_{0,ee}$ corresponding to pose 1 of Table 2 (with zero θ's) are

$$\mathbf{A}_{F200,ee} = \begin{bmatrix} -0.0228 & 0.57961 & -0.8146 & -366.5600 \\ 0.0215 & -0.8143 & -0.5800 & -12.6340 \\ -0.9995 & -0.0307 & 0.0061 & -107.7100 \\ 0 & 0 & 0 & 1 \end{bmatrix} \tag{14}$$

$$\boldsymbol{A}_{0,ee} = \begin{bmatrix} 1 & 0 & 0 & 1209.25 \\ 0 & 1 & 0 & 0 \\ 0 & 0 & 1 & 0 \\ 0 & 0 & 0 & 1 \end{bmatrix} \tag{15}$$

Table 2 Six poses of wire-actuated manipulator used for identifying $\boldsymbol{A}_{0,F200}$.

Pose #	Pitch (rad)	p_x (mm)	p_y (mm)	p_z (mm)
1	0	1209.2500	0	0
2	–1.5708	1090.6500	–118.6000	0
3	–0.5236	1128.6846	–300.6746	0
4	–0.5236	1193.3606	–59.3299	0
5	0	1127.8071	303.9496	0
6	–1.5708	1009.2071	185.3496	0

The calculated constant pose (roll, pitch, yaw rotations and the three translational coordinates) of the F200*i* tool with respect to the base frame of wire-actuated manipulator for the six poses are averaged to obtain $\boldsymbol{A}_{0,F200}$ as

$$\boldsymbol{A}_{0,F200} = \begin{bmatrix} 0.0040 & -0.0112 & -0.9999 & 1091.308 \\ 0.5814 & -0.8135 & 0.0114 & 218.248 \\ -0.8136 & -0.5814 & 0.0033 & -302.304 \\ 0 & 0 & 0 & 1 \end{bmatrix} \tag{16}$$

As well, a root-mean-square minimization is applied on the roll-pitch-yaw Euler angles and position coordinates and the resulting $\boldsymbol{A}_{0,F200}$ is very close to its expression in (16). The transformation

matrix $\boldsymbol{A}_{0,F200}$ is used for transferring an additional 100 measured poses of the wire-actuated manipulator to its base frame.

Two sets of data are collected during the measurement process; one using the data acquisition board (four encoder readings) and one based on the Polaris tracking system. Because of the time lag between the two measuring devices, and also since the data acquisition collects data for the whole duration of the data collection process while Polaris measurements are only for the discrete poses, some manipulation (filtering, analysis and reformatting) of data are required before they could be ready for the identification process. The processed data are transferred to the manipulator base frame before they are used in the calibration program developed for [4].

Table 3 lists the parameters that are kept constant during calibration, where $\delta\theta$ represents the constant error (offset) in displacement of joint i and l_1 is the link length between joints two and seven (j_2 and j_7 in Figure 1). The results are reported in Table 4 (root-mean-square errors before and after calibration) and Table 5 (nominal and identified values of parameters) for both GN and LM methods. As it can be seen from Table 4, for both methods the root-mean-square errors in translation and rotation have been reduced by 25% and 35% respectively. These results are very encouraging as during measurements many errors were introduced. For example, all the four encoders are relative (incremental) type and they need a reference position for their readings. At the start of tracking, the rigid branch of the manipulator was positioned as close to its zero-configuration (when all revolute joints have zero rotation) as possible and then the readings of the encoders were recorded relative to this configuration. As well, to identify the constant transformation from the base of the wire-actuated parallel manipulator to the tool on F200*i*, the rigid branch was moved to the known poses as close as possible and the transformation was calculated based on the nominal values of parameters. For further improvements in the calibration results, the entries in $\boldsymbol{A}_{0,F200}$ could be updated iteratively based upon the updated parameters from the calibration program.

Table 3 Parameters kept constant during calibration.

Parameter	Value (rad or mm)
$\delta\theta_0$	0.0
$\delta\theta_3$	0.0
d_1	104.85
$d_{3'}$	–104.85
a_1	0.0
l_1	209.7

Table 4 Root-mean-square errors of mobile platform pose (100 poses).

	Initial	Final (GN)	Final (LM)
RMS Error - Translation (mm)	22.828	17.194	17.191
RMS Error - Orientation (rad)	0.0591	0.0382	0..0383

Table 5 Nominal and identified parameters of rigid branch for 100 poses.

Parameter	Nominal	Identified (GN)	Identified (LM)
$\delta\theta_1$	0.0	0.0213	0.0214
$\delta\theta_2$	0.0	0.0200	0.0201
$\delta\theta_4$	0.0	–0.0551	–0.0548
$\delta\theta_5$	0.0	–0.0425	–0.0411
a_0	0.0	–3.186	–3.216
a_2	607.900	601.211	601.620
a_3	0.000	0.341	–0.062
a_4	482.750	494.437	494.340
a_5	118.600	118.433	118.459
α_0	0.0	–0.0326	–0.0325
α_1	1.5708	1.5743	1.5741
α_2	0.0	–0.028	–0.0281
α_3	0.0	0.0733	0.0734
α_4	0.0	0.0001	–0.0003
α_5	0.0	0.0298	0.0294
β_0	0.0	–0.0023	–0.0020
β_2	0.0	0.0061	0.0055
β_4	0.0	0.0127	0.0121
β_5	0.0	–0.0153	–0.0152
l_3	209.700	206.902	206.859
l_4	607.900	599.193	599.648

5. CONCLUDING REMARKS

This article concentrated on the experimental calibration of the constraining linkage (rigid branch) of a wire-actuated parallel manipulator. The manipulator utilizes redundancy in sensing (in addition to redundancy in actuation); hence all the independent joints of the rigid branch are sensed. This enables calibration of the rigid branch independent from the wire mechanism, as the pose of the mobile platform could be calculated utilizing the readings of the two actuated joints and the two sensed passive joints of the rigid branch. Preliminary results have been very encouraging taking into account the measurement

errors for the reference pose of relative encoders, and also for the known configurations of the rigid branch that were used for identifying the constant transformation from the base frame of wire-actuated manipulator to the F200*i* frame. Currently the calibration of the wire mechanism, based on the mobile platform pose error, is underway as an undergraduate fourth-year thesis project.

REFERENCES

1. Roth, Z.S., Mooring, B.W., and Ravani, B., Overview of Robot Calibration. *IEEE Trans. Robotics and Automation*, 3(5):377-385, 1987.
2. Mooring, B.W., Roth, Z.S., and Driels, M.R., *Fundamentals of Manipulator Calibration*, John Wiley & Sons, 1991.
3. Mroz, G., and Notash, L., Design and Prototype of Parallel, Wire-Actuated Robots with a Constraining Linkage, *J. Robotic Systems*, 21(12):677-687, 2004.
4. Varziri, M.S., and Notash, L., Kinematic Calibration of a Wire-Actuated Parallel Robot, *Mechanism and Machine Theory* (in print).
5. Paul, R.P., *Robot Manipulators: Mathematics, Programming, and Control; the Computer Control of Robot Manipulators*, MIT Press, 1981.
6. Notash, L., Podhorodeski, R.P., Fixturless Calibration of Parallel Manipulators, *Transactions of the CSME*, 21(3):273-294, 1997.
7. Polaris System User's Guide, Version 1.0, Northern Digital Inc., 2002.
8. Press, W.H., Teukolsky, S.A., Vetterling, W.T., and Flannery, B.P., *Numerical Recipes in C*. Cambridge University Press, 1992.
9. NDI 6D Architect User's Guide, Version 1.0, Northern Digital Inc., 2003.